Wet size measurements for the evaluation of the deagglomeration behaviour of spray-dried alumina powders in suspension

Antoine Marie, Mallorie Tourbin, Anne-Charlotte Robisson, Carine Ablitzer, Christine Frances

Author Accepted Manuscript for publication
Paper published in:

Ceramics International
Volume 48, Issue 6, 15 March 2022, Pages 7926-7936
https://doi.org/10.1016/j.ceramint.2021.11.340

Wet size measurements for the evaluation of the deagglomeration behaviour of spray-dried alumina powders in suspension

Antoine Marie[1], Mallorie Tourbin[2], Anne-Charlotte Robisson[1], Carine Ablitzer[1], Christine Frances[2]

[1] *CEA, DES, IRESNE, DEC, Cadarache F-13108 Saint-Paul-Lez-Durance, France*
[2] *Laboratoire de Génie Chimique, Université de Toulouse, CNRS, INPT, UPS, Toulouse, France*

**Corresponding author:* anne-charlotte.robisson@cea.fr
Postal address : CEA Cadarache, Sait-Paul-Lez-Durance, France

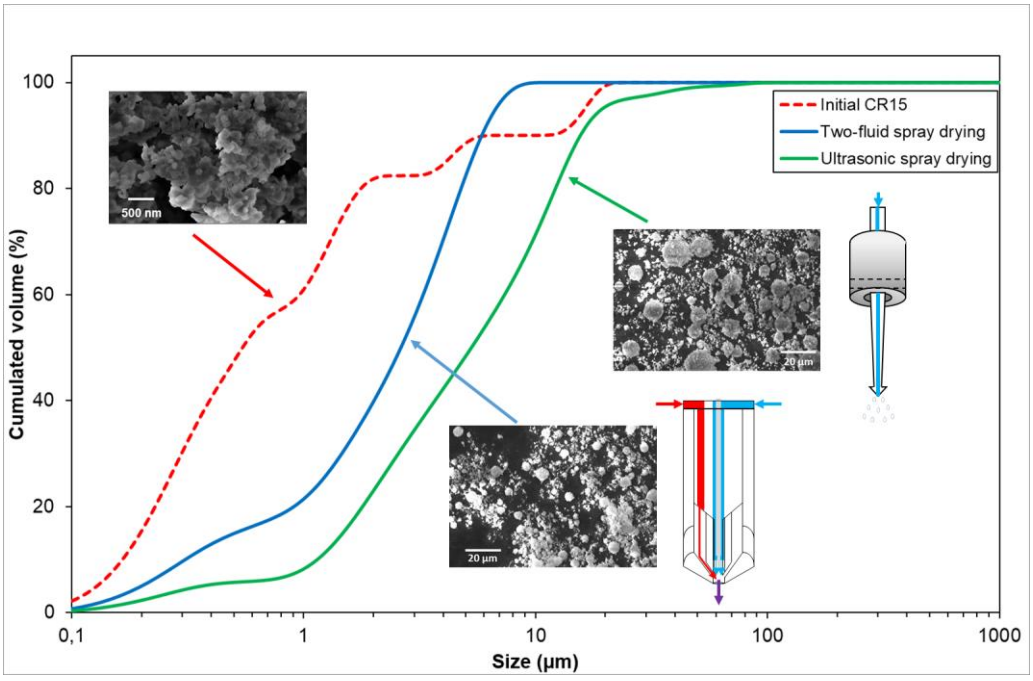

Wet size measurements for the evaluation of the deagglomeration behaviour of spray-dried alumina powders in suspension

Antoine Marie[1], Mallorie Tourbin[2], Anne-Charlotte Robisson[1], Carine Ablitzer[1], Christine Frances[2]

[1] *CEA, DES, IRESNE, DEC, Cadarache F-13108 Saint-Paul-Lez-Durance, France*

[2] *Laboratoire de Génie Chimique, Université de Toulouse, CNRS, INPT, UPS, Toulouse, France*

**Corresponding author:* anne-charlotte.robisson@cea.fr

Postal address : CEA Cadarache, Sait-Paul-Lez-Durance, France

Abstract

Spray drying produces spherical agglomerates to obtain powders with good flowability. Three alumina powders of different size and/or specific surface area were spray-dried without any binder using either two-fluid or ultrasonic nozzle technology. Compared to the two-fluid nozzle, the ultrasonic one shows a better ability to form agglomerates from a coarse powder and increases the size of the agglomerates when spray drying is carried out under the same operating conditions. The redispersion of spray-dried agglomerates in solution was analysed by applying variable ultrasound durations during size measurement by wet laser diffraction. The initial state of the powder plays a predominant role in relation to the spray drying operating conditions both in terms of size characteristics and redispersion properties. Regardless of the alumina powders and spray drying conditions, a similar trend in deagglomeration behaviour was observed with first-order kinetics and a characteristic kinetic time depending on the initial powder properties.

Keywords: spray-drying**,** ultrasonic nozzle, two-fluid nozzle, alumina, deagglomeration, dispersion

1. Introduction

Ceramics, such as alumina, are widely used as refractory materials, electrical insulators or sintered parts in a wide variety of fields, including aeronautics, medicine, energy and many others. Different steps are necessary for their shaping such as mould filling, pressing and sintering. The correlation between sintering behaviour and compacted pellet properties has been studied for years [1-4], demonstrating the influence of powder agglomeration into the pellets. To enhance the filling behaviour, it is also important to control the flowability of powders, which impacts the compaction of the pellets [5-6].

Spray-drying is a well-known technique used to produce spherical agglomerates, which were proved to increase the powder flowability and consequently enhance compaction [7-9] . This allows obtaining the powder required properties (flowability, size distribution and particle shape) and, hence, improving compaction behaviour [10-11].

The main parameters that influence the morphology and size distribution depend on the spray drying technology, but they are basically the same: slurry properties (e.g. solid concentration, initial particles, surface tension or suspension viscosity) and process parameters (e.g. gas temperature and flow rate, slurry feed rate, air pressure of spraying gas or air moisture). It has been shown that agglomerate size is affected by droplet size, slurry concentration and initial particle size, whereas initial particle size distribution and agglomeration in the slurry will affect morphology [12-16]. For example, concerning the spray-drying of hydroxyapatite, Wang et al. [12] noticed a significant effect of the air flow rate on the granule size: granule size increases with decreasing air flow rate but with a less pronounced effect when the slurry feed rate is higher.

These general observations were also noted by several authors on alumina powders. Minoshima et al. [17] examined the effect of droplet diameter and slurry concentration, and found that increases in both parameters resulted in the production of larger agglomerates. In addition, Bertrand et al. [18] used suspensions at different pH, and thus in different dispersion states. Suspensions at pH 4 were

flocculated whereas at pH 9 they were well dispersed. It appears that alumina suspensions at low pH gave dense and spherical-shaped agglomerates when spray-dried whereas suspensions at pH 9 lead to hollow granules. They correlated this behaviour to the difference between the mobility of the solid particles in the suspension and during the drying process. Ramavath et al. [7] studied the flowability of spray-dried alumina, starting with a submicronic powder. They used slurries with different solid alumina contents and found changes in average agglomerate size (higher concentration leads to larger average agglomerate size). Flowability measurements also showed a significant reduction in the cohesion index between the initial powder and the spray-dried powders, with values corresponding to "very cohesive" for the initial powder and "free flowing" for the spray-dried powders, based on data provided by the manufacturer of the powder flow analyser. Choudhary et al. [19] also spray-dried submicronic alumina, and examined both the concentration and feed rate of the suspension. They found a significant effect of these parameters on the shape and size distributions of agglomerates, observing shape degradation with high feed rates (above 5 $mL.min^{-1}$) for low-viscosity suspensions. Yu et al. [20], who further evaluated the spray-drying parameters (inlet temperature, slurry concentration, feed rate), reached the same conclusion as Ramavath et al. [7] concerning the influence of temperature and feed rate on agglomerate size. The influence of inlet temperature is more complex to assess. Granule size grows with increasing temperature up to a maximum, beyond which the evaporation time of the droplets is so short that the agglomerates systematically explode in the drying chamber.

In addition, several authors have studied spray-drying applied to alumina powders using organic binders. Frey and Halloran [21] related the density after compaction to different properties of spray-dried alumina (granule size, moisture content and binder concentration). It is pointed out that an augmentation of binder concentration increases moisture content of spray-dried powder, and that higher moisture content results in green compacts of higher density. Granule size has less influence on moisture content. Baklouti et al. [22] also analysed the compaction behaviour of spray-dried alumina with organic binders, focusing on the influence of the binder nature on the resistance of the granules to compaction-induced mechanical deformation. At a glance, Stunda-Zujeva et al. [23] proposed an Ishikawa diagram which summarizes the factors influencing shape and size distribution of spray-dried powders.

Another key factor in spray drying process is the nozzle technology (rotary or disk nozzles, hydraulic or pneumatic nozzles, ultrasonic devices). In particular, two-fluid nozzles are widely used in laboratory-scale spray-driers. It is known that the flow rate of the drying gas (assimilated to the energy of spray-drying) affects the droplet size [24-26].

More recently, a spray-drying nozzle was developed by Sono-Tek Corporation (USA) in collaboration with Büchi Labortechnik AG (Switzerland), a manufacturer of laboratory scale spray dryers. It is an ultrasonic nozzle, which represents an alternative to the conventional nozzles, allowing low-speed spraying. Several advantages have already been noted, such as better control of droplet size and the ability to avoid clogging [27-28]. In addition, the risk of agglomerate shrinkage in the drying chamber is limited by the lower mechanical stress caused by the ultrasonic vibration on the droplets [27]. A few works has focused on the feasibility of spray-drying with an ultrasonic atomizer for different materials (proteins, polymers, biomaterials), mainly for the purpose of encapsulation [27, 29-32].

Moreover, the handling and manutention of powders are rather common in industrial processes. These steps, applying stress to agglomerates and forcing particles to collide other particles can lead the powders to deagglomerate. Characterization of the rate of deagglomeration is important to quantify the strength of agglomerates and to assess, for example, the ability of a powder to produce dust. Various techniques and methodologies have been used to characterize the deagglomeration behaviour and/or the agglomerate strength. Schneider and Jensen [33] proposed for instance a method aiming to study dustiness, combining a single drop and a rotating drum test. Jaffari et al. [34] worked with dry laser diffraction analysis to determine the ease of deagglomeration and cohesion of pharmaceutical powders by varying dispersion pressure from 0.2 to 4.5 bar. Kurkela et al. [35] developed a specific apparatus to measure the deagglomeration of powders in a steady and well

controlled turbulent gas flow system and related the degree of deagglomeration with the flow characteristics. In addition, the experimental analysis and simulation of agglomerate breakage by impact have been described extensively in the literature [36-38]. The analysis of the redispersion of agglomerated powders in liquid medium is another challenging question. The ability to redisperse in a liquid is a function of the nature of the interparticle bonds, the surface charges and the physico-chemical properties of the suspension. Mahr and Halbedel [39] related for example the deagglomeration behaviour of nanoscaled barium hexaferrite powders with the zeta potential and the pH of the suspension. Wet deagglomeration can be performed using many types of equipment such as rotor-stators, high pressure nozzles devices or milling systems which can generate high mechanical stresses. Such processes are well adapted for very cohesive agglomerates, but poorly cohesive systems can be dispersed in tanks applying moderate agitation and/or ultrasound. The application of ultrasound in water as a deagglomeration tool was carried out by Wang et al. [40] on aluminium alloys in order to explore the fragmentation mechanisms. Kudryashova et al. [41] developed a model to describe the dynamics of nanoparticles behaviour in a liquid metal with the application of ultrasound which can either cause the particles to coagulate or deagglomerate.

Some authors have proposed to characterize the deagglomeration behaviour in dry or wet conditions, expressing a relative deagglomeration index [42-43]. These indexes are often based on size distribution measurements. Schuck et al. [42] proposed for example a relative deagglomeration expression derived from dry laser diffraction analysis, varying the dispersion pressure of the feeding system. This index *F* is defined as follows by the equation (1):

$$F = \left(\frac{d_{50}(50\ kPa) - d_{50}(400\ kPa)}{d_{50}(50\ kPa)} \right) * 100 \quad (1)$$

Where $d_{50}(x\ kPa)$ corresponds to the volume median size d_{50} measured at a dispersion pressure of *x kPa*.

Parisini et al. [43] also used dry laser diffraction analysis, to define a deagglomeration index y based on an empirical model fitting the mono-exponential curves they obtained. Their equation is derived from JMAK (Johnson-Mehl-Avrami-Kolmogorov) equation, usually used for granulation or phase changes kinetics [44]:

$$y = m * \left(1 - e^{-(x/x_0)^n}\right) \quad (2)$$

Where x_0, m and n are fitting parameters. x_0 is a characteristic value related to the x-axis variable, m corresponds to the maximum deagglomeration and n is the deagglomeration exponent.
In this context, the aim of the present work consists in analysing the effect of the spray-drying process on the characteristics of the agglomerates produced without any binder and more particularly on their ability to deagglomerate in aqueous medium. Alumina has been chosen due to its physico-chemical properties (availability of size range and ability to aggregate). Characterizations such as SEM and wet laser diffraction analysis were carried out to observe the effects inducted by the spray-drying conditions. The objective of this paper is twofold: i) to determine a simple way to characterize deagglomeration in water and quantify the degree of deagglomeration and ii) at the same time to discuss the impact of the use of an ultrasonic nozzle compared to a more conventional bi-fluid nozzle on the characteristics of agglomerated powders.

2. Materials and methods

2.1. Materials and properties

Three high purity alumina powders from the Baïkalox® range provided by Baïkowski were used for this study: CR6 and CR15 that are jet-mill deagglomerated powders and GE15 which is an unground powder.

Scanning Electron Microscopy (SEM) was used to observe particle morphology using a FEI Nova Nano SEM with secondary electrons (SE) and a voltage of 5 kV. The SEM pictures (cf. Figure 1) show rough shapes for all powders, but a distinction in particle size can already be made. At a large magnification (x 100 000), it can be seen that all the three powders are constituted by primary particles having similar shape and size of about 150 nm wide by 300 nm long. However, at a low magnification (x 500), pictures show that the CR6 (Figure 1a) and CR15 (Figure 1b) powders are mainly composed of fine aggregates of a few microns and large agglomerates of a few hundred microns in size which may have agglomerated naturally, whereas the GE15 powder (Figure 1c) presents individual larger aggregates having irregular shapes of a few tens of microns. This is most likely a result of the different methods used to produce these powders.

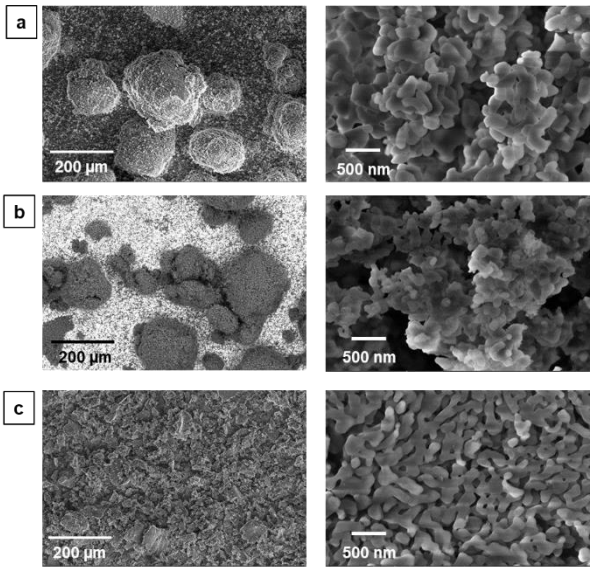

Figure 1: SEM pictures of initial powders using magnification x 500 (left) and x 100 000 (right) (a: CR6, b: CR15, c: GE15)

Nitrogen adsorption/desorption isotherms were also performed to characterize the textural properties of the samples with an ASAP 2460 instrument (Micromeritics). Specific surface areas (SSA^{BET}) were determined from the linear portion of the Brunauer-Emmet-Teller (BET) plots. The measured SSA^{BET} of the three raw powders are summarized in Table 1.

Measured data	**CR6**	**CR15**	**GE15**
ρ (g.cm^{-3})	3.979 ± 0.005	3.930 ± 0.004	3.943 ± 0.015
d_{50} (µm)	0.72	0.49	17.62
d_{32} (µm)	0.54	0.36	4.14
SSA_{th} (m².g^{-1})	*2.79*	*4.24*	*0.37*
SSA^{BET}(m².g^{-1})	5.7 ± 0.2	14.1 ± 0.2	13.8 ± 0.2
$d_{p\ (nm)}$	*264*	*108*	*110*

Table 1: Measured characteristics of the raw powders

Moreover, the size distributions of the powders were measured by laser diffraction with a LS13 320 analyser (Beckman Coulter) in wet way. Alumina particles do not dissolve because this compound is qualified as non-soluble in water (at 20°C). Initial alumina dispersions were characterized through potential zeta and pH measurements (Table 2). The pH values for the three dispersions are identical and consistent with that of tap water. Potential zeta values are in agreement with those reported in the literature for such suspensions [45]. They show a good stability of the dispersions for the CR6 and CR15 powders, and a rather poor stability for the GE15 dispersion since its zeta potential is about 14.9 mV, and thus below the limit of 25 to 30 mV, generally characterising a stable dispersion. Figure 2 shows the size distributions of the initial powders when an ultrasonic treatment is applied prior to the wet diffraction measurement to better disperse the powder. Powders containing agglomerates disperse under the effect of ultrasound and the size distribution shifts slightly towards smaller sizes when the duration of the ultrasound treatment is increased. It can be noted that CR15 and CR6 powders have an offset distribution towards the small sizes compared to GE15 powder and that agglomerates around 100 µm observed by SEM analysis are probably destroyed after dispersion in water for size distribution measurements. In accordance with the SEM images, these powders consist of aggregated particles of few microns that are smaller than GE15 powder. For the GE15 powder, the large aggregates, visible by SEM analysis of a few tens of microns or even up to a hundred microns, are hardly dispersed. This may be due to the fact that the low surface potential does not allow to counterbalance the attractive forces and explain why the ultra-sonication does only have a small effect on the GE15 powder dispersion.

The median size and the Sauter diameter measured after 5 minutes of ultrasound application are reported in Table 1. The Sauter diameter [46] is defined as the ratio of the third order moment of the population density to the second order moment :

$$d_{32} = \frac{\sum_i n_i \, x_i^3}{\sum_i n_i \, x_i^2} \qquad (3)$$

where n_i is the population density of particles or aggregates having a size x_i.

Assuming that the particles are spherical, the Sauter diameter and the specific surface are inversely proportional :

$$SSA_{th} = \frac{6}{\rho d_{32}} \qquad (4)$$

where ρ is the true material density. Its value has been measured by Helium pycnometry (Micromeritics AccPyc 1330 Pycnometer) for the three powders. The values obtained, reported in Table 1, are very close to each other and to the reference value for alumina (3.95 $g.cm^{-3}$).

The accuracy of the size mean values are about 0.02 µm. Thus, it can be noted that CR6 and CR15 powders have a similar median size and a different specific surface area, while CR15 and GE15 powders have a similar specific surface area and a quite different size range. Furthermore, assuming that the alumina particles are perfectly smooth and spherical, and considering the measured true material density for each powder, the theoretical specific surface area of the powders (SSA_{th}) can be calculated from the Sauter diameter. This would be equal to 2.79, 4.24 and 0.37 m^2/g respectively for CR6, CR15 and GE15 powders to be compared with the BET specific surface area values given in the Table 1. It can be concluded that the particles are highly porous and agglomerated, in particular GE15 powder (and to a lesser extent CR15 and CR6 powders). The measured specific surface areas are more probably those of the primary particles constituting the aggregates. With the assumption that the specific surface measured by the BET method is the specific surface of the primary particles, the equation (4) can be used again to estimate the primary particle sizes. The calculated values of the primary particle size, also reported in table 1, are respectively of 264, 108 and 110 nm, respectively for CR6, CR15 and GE15 powders. The agglomeration factor (i.e. the number of primary particles in the aggregates) can be evaluated. The number of primary particles is equal to the ratio of the diameters of the agglomerate to that of the primary particles raised to the power of three. This number is about 8 and 37, respectively

for CR6 and CR15 powder but may reach about 50.10^3 for the GE15 powder. However, this result must be taken with caution given the assumptions about the sphericity of the particles.

	ZP (mV)	Average ZP (mV)	pH
CR6	30.7	30.8	5.93
	30.0		
	31.6		
GE15	14.5	14.9	5.98
	16.4		
	13.9		
CR15	31.8	33.4	5.98
	34.4		
	34.0		

Table 2: Zeta potential (ZP) and pH measurements of alumina suspensions in water before spray-drying

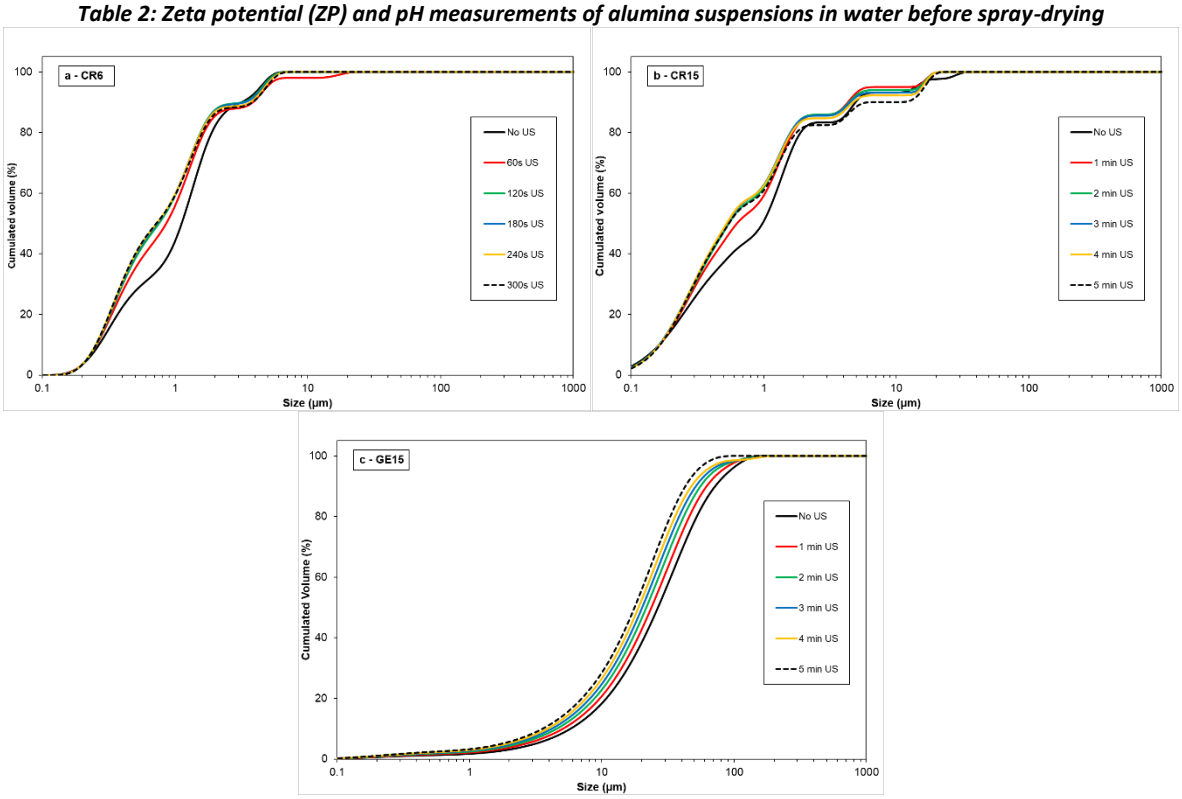

Figure 2: Size distributions of initial powders function of ultrasonic treatment duration (a: CR6, b: CR15, c: GE15)

2.2. Spray-drying nozzle technologies

In this study, a laboratory scale Mini Spray-Dryer B290 (Büchi, Switzerland) was used to shape alumina agglomerates. This model offers two types of nozzles [47]: a two-fluid nozzle with an orifice diameter of 0.7 mm, which is fairly "conventional" – producing droplets smaller than 20 µm in size [48] – and a less common ultrasonic nozzle, which produces droplets averaging 31 µm in size (data provided by SonoTek, manufacturer of ultrasonic nozzle [49]). Both nozzles are shown in Figure 3. In the two-fluid nozzle, suspension enters in the duct where it meets pressurized air which pushes the fluid through the orifice. This gives shape to the droplets which are dried by the hot drying gas in the spray-drying chamber. The way droplets are produced is different with an ultrasonic nozzle. Ultrasound cause the atomizing surface to vibrate, producing a film of suspension that spreads over the atomizing surface

and generates capillary waves when it absorbs the vibrations. These waves then collapse and eject the droplets into the drying chamber [29].

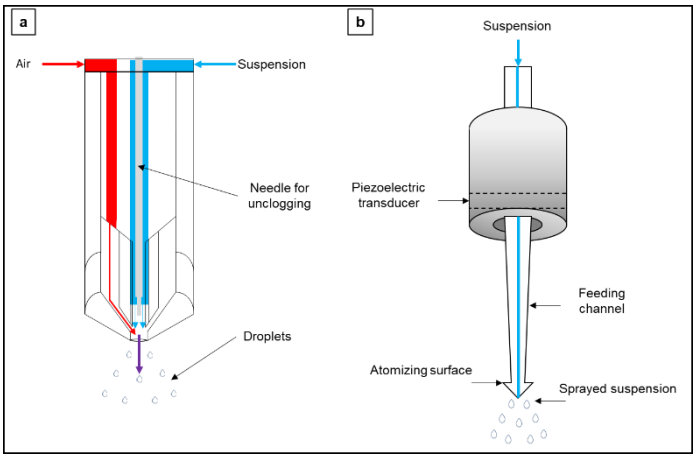

Figure 3: Spray-dryer nozzles (a: two-fluid nozzle, b: ultrasonic nozzle)
In blue: fluid (suspension or solution), in red: pressurized air mixed with suspension

2.3. Spray-drying experiments

Slurries of different solid contents were prepared by mixing tap water and alumina powders, without any binder or dispersant. Before and during spray drying, the suspension was kept mixed using a magnetic stirrer.

Run label	Nozzle type	Temperature (°C)	Feed rate ($L.h^{-1}$)	Concentration ($g.L^{-1}$)	Gas flow rate ($m^3.h^{-1}$)	Spraying gas pressure (bar)	Ultrasonic nozzle power (W)
Tf1 – CR6	Two-fluid	120	0.3	30	38	7	X
Tf1 – CR15							
Tf1 – GE15							
Tf2 – CR15	Two-fluid	120	0.6	30	30		
Tf3 – CR15	Two-fluid	120	0.6	60	38		
Tf4 – CR15	Two-fluid	150	0.6	30	38		
Tf5 – CR15	Two-fluid	150	0.6	60	38		
Us1 – CR6	Ultrasonic	120	0.3	30	38	X	2
Us1 – CR15							
Us1 – GE15							
Us2 – CR15	Ultrasonic	140	0.6	30	38		
Us3 – CR15	Ultrasonic	140	0.3	30	38		

Table 3: Spray-drying operational conditions performed with alumina powder

Spray-drying tests were performed on all the three powders in order to better understand the effect of the initial properties of the alumina powders and the spray-drying process parameters on the agglomeration of the particles with the two nozzles (cf. Table 3). The results will be presented and discussed more in details concerning the CR15 powder for which the considered parameters were the slurry solid concentration, the feed suspension flow rate, and the drying gas temperature and flow rate.

3. Results – discussion

3.1. Two-fluid nozzle - Powder influence

This section presents the results obtained in the case study of the Tf1 experiment with the two-fluid nozzle and the following conditions: temperature 120°C, slurry concentration 30 $g.L^{-1}$, feed rate 0.3 $L.h^{-1}$, drying gas flow rate 38 $m^3.h^{-1}$. The behaviour of the three alumina powders under these spray-drying conditions was evaluated. Figure 4 shows the cumulated size distributions of the three powders before and after spray-drying, without ultrasound application during the wet size measurements. Several points should be noted: the average sizes of CR15 and CR6 increase relatively significantly with spray-drying (from 0.72 and 0.49 µm respectively to about 5 µm). Conversely, GE15 powder, which was initially larger, did not agglomerate during spray-drying. There was even a slight decrease in the median size, probably due to particle handling, which induced a dispersion of the larger aggregates, initially present in the powder. The poor stability of GE15 powder in water, characterised by a zeta potential value of 14.9 mV, may also induce agglomeration of the particles present in the initial suspension and explain why the initial size of GE15 in water is bigger than the size of the spray-dried particles.

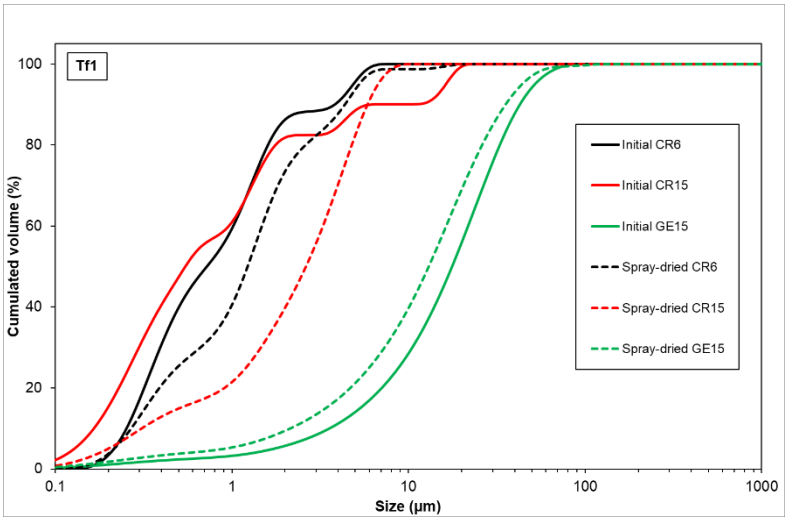

Figure 4: Comparison of the powder size distributions before and after spray-drying (Tf1 conditions)

In accordance with the particle size measurements, the SEM pictures (Figure 5) reveal that in fact GE15 (Figure 5c) powder is simply not spray-dried but only dried, i.e. spray-drying does not agglomerate the powder into spherical particles, unlike CR6 (Figure 5a) and CR15 (Figure 5b) powders. However, for CR6 and CR15, agglomeration seems to be incomplete since many submicronic particles and aggregates are not agglomerated. About the agglomerates sizes, these pictures show agglomerates with approximate size in agreement with the size distributions measured.

The deagglomeration ability of the spray-dried powders was achieved by wet particle size analysis using ultrasound of variable duration, applied with a probe (whom maximum power is 73W). By this way, deagglomeration is forced by applying stress to the particles: once suspended in water with a naphtalene-based dispersant (Daxad® 15, provided by GEO – 1 $g.L^{-1}$, used to improve the dispersion of particles in water and avoid their re-aggregation), ultrasound was applied to the suspension in order to "destroy" the agglomerates. Several durations were considered: 15 s, 30 s, 1 min, …, up to 10 min. The measurements were successive: 30 s corresponds to a total ultrasound application of 15 s, then 15 s more.

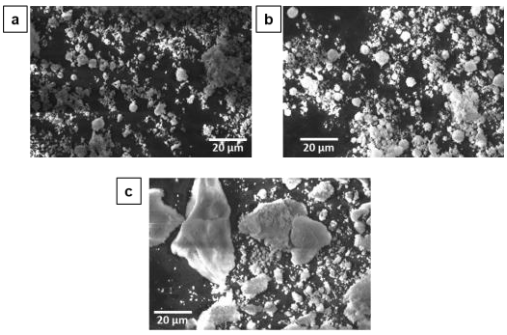

Figure 5: SEM pictures of powders spray-dried in Tf1 conditions using the two-fluid nozzle (a: CR6, b: CR15, c: GE15)

Gradual deagglomeration was observed by increasing the duration of ultrasound application (Figure 6). This deagglomeration behaviour should be related to that of the initial CR15 powder (Figure 2b), for which virtually no deagglomeration was observed under ultrasonic conditions. The progressive deagglomeration of spray-dried CR15 is noteworthy with the evolution of cumulated particle size distributions: the population of agglomerates around 4 µm gradually disappears in favour of submicronic particles. This reflects the dispersion of CR15 agglomerates obtained by spray-drying under stress caused by the application of ultrasound in a wet environment. The main change for this powder occurs during the first two minutes of ultrasound application, where a major population of submicronic particles is noticed. The particle size distribution of CR15 containing about 65% of submicronic particles no longer evolves after 180 s of ultrasound application, and almost no further deagglomeration occurs. Overall, the dispersion of the agglomerates is almost complete as only 10% of the agglomerates larger than 4 µm remain at the last measurement.

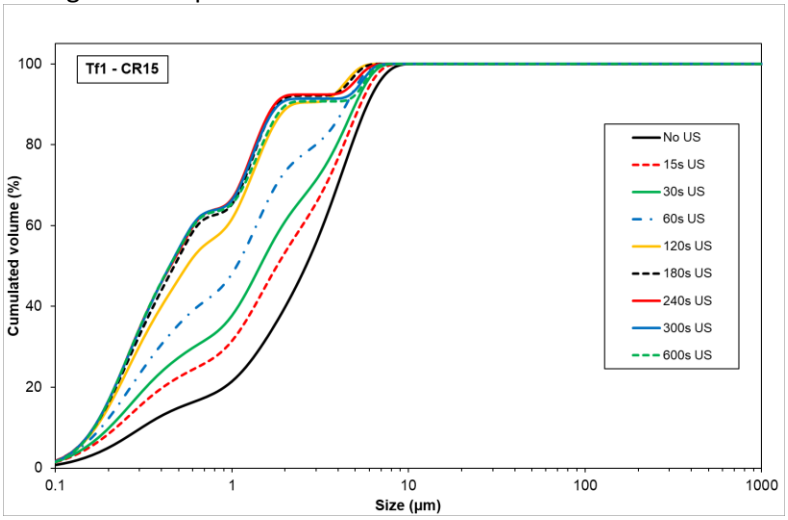

Figure 6: Impact of ultrasound application on the dispersion of CR15 powder spray-dried (Tf1 conditions): evolution of size distribution

To see more clearly, the deagglomeration behaviour is analysed through the variation of the d_{10}, d_{50} and d_{90} diameters in function of ultrasound application time. Figure 7 also presents the repeatability of measurements on these characteristic diameters (experiment Tf1 - CR15 was performed twice). There is good overall agreement for the values d_{50} and d_{10}. On the other hand, significant differences can be observed for the values of d_{90}. This can be explained by the appearance of agglomerates that form randomly. Overall, it can be concluded that the spray drying experiments and the deagglomeration of powders in the wet laser diffraction analysis have good repeatability. Moreover, this shows a stabilisation of d_{10} starting from 120 s and d_{50} and d_{90} starting from 240 s.

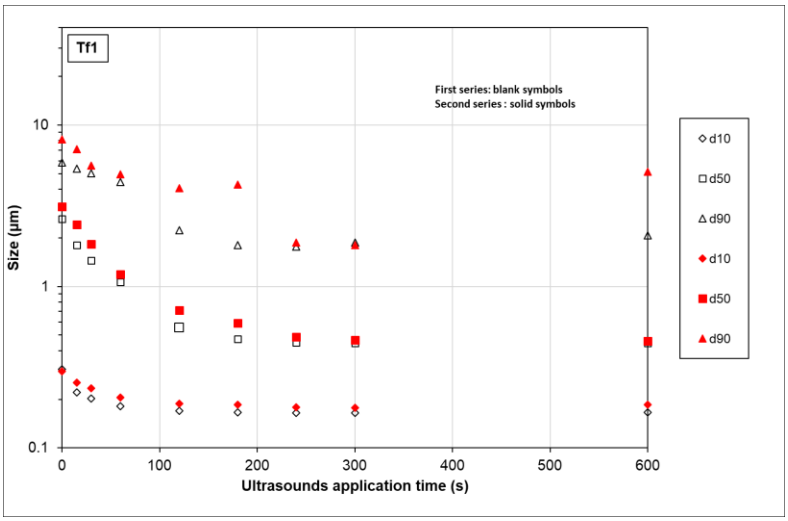

Figure 7: Change of d_{10}, d_{50} and d_{90} of CR15 powder spray-dried vs ultrasound application time (Tf1 conditions)

Spray-drying of all three powders (CR6, CR15, GE15) was carried out under the same conditions Tf1 (the impact of ultrasound application on the evolution of size distribution on CR6 powder is reported in the supplementary material, Figure S1). Figure 8 shows the evolution of d_{10}, d_{50} and d_{90} for the three spray-dried powders. These results show that the initial size distribution influences the deagglomeration behaviour of the spray-dried powders. Indeed, the diminution of d_{10}, d_{50} and d_{90} for the CR6 and CR15 powders indicates a deagglomeration whereas the GE15 powder has a fairly constant size and therefore limited deagglomeration. Moreover, for the CR6 powder, the d_{50} value becomes stable earlier under ultrasound application (after about 180 s) than for the CR15 powder (for which the d_{50} stabilizes after about 240 s).

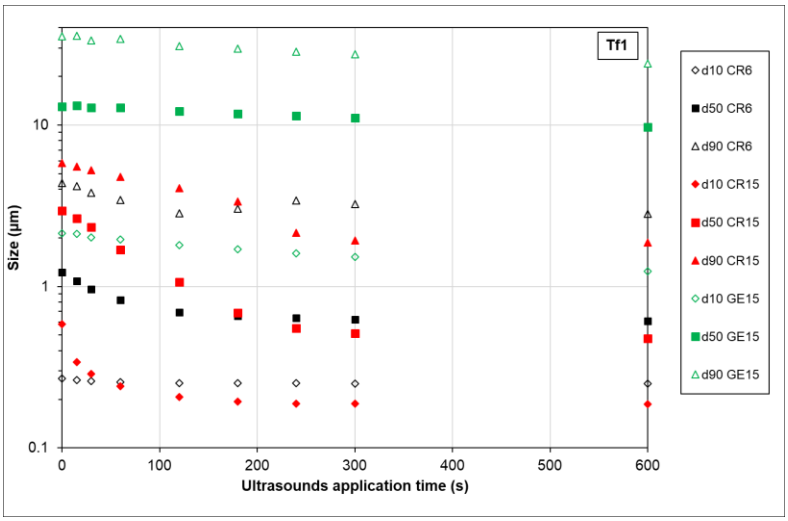

Figure 8: d_{10}, d_{50} and d_{90} evolution for the three powders spray-dried with the two-fluid nozzle (Tf1 conditions)

In addition, the change in median size as a function of ultrasound application time for all tests carried out on CR15 powder with the two-fluid nozzle is reported in the supplementary material (see Figure S2). In summary, the difference induced by the parameters (temperature, slurry feed rate, slurry concentration) – within the ranges studied – seems small. Indeed, they do not drastically affect either the particle size distribution of the collected spray-dried powders because, for each spray drying condition tested, the measured d_{50} remains very close, between 2 and 3 µm. Furthermore, in these five spraying conditions, the deagglomeration profiles present the same behaviour with constant d_{50} values from 240 s of ultrasound application time.

3.2. Ultrasonic nozzle – Powder influence

Figure 9 shows the cumulated size distributions of the three powders before and after spray-drying with the ultrasonic nozzle using Us1 conditions. The measurements were done without additional ultrasound application. Figure 10 reports SEM pictures of the three alumina powders spray-dried with the ultrasonic nozzle under Us1 conditions. Compared to the powder collected after spray-drying with the two-fluid nozzle under operating conditions equivalent to Tf1 conditions (Figure 5), two major differences are noticeable: the change in size distribution for CR15 and CR6 powders with the formation of larger agglomerates (Figure 9), also shown in SEM photos (Figures 10a and 10b) and the formation of spherical agglomerates under Us1 conditions for GE15 powder (Figure 10c). If the change of morphology for GE15 is strong, the change in particle size distribution of the GE15 powder (cf. Figure 9) is not so obvious. The average size of the spray-dried powder is even smaller than the initial powder observed by SEM. This is probably the result of the disintegration of the larger aggregates initially present in the powder during the pumping and dispersing steps in the spray nozzle.

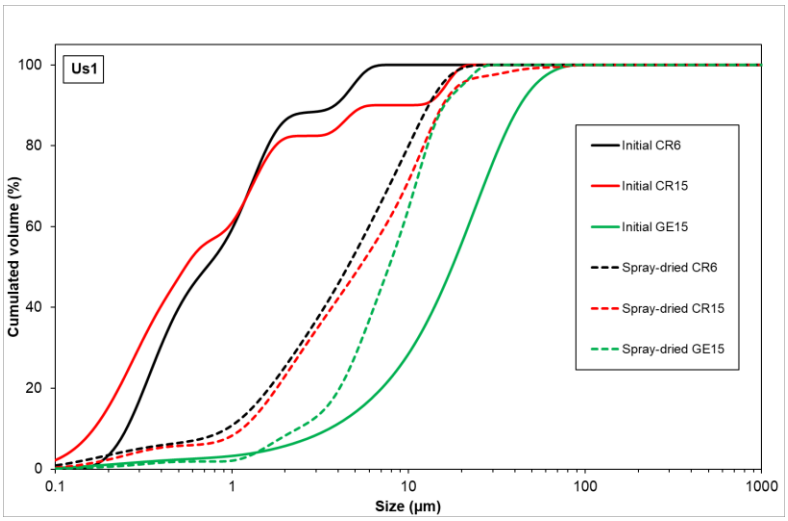

Figure 9: Comparison of the powder size distributions before and after spray-drying (Us1 conditions)

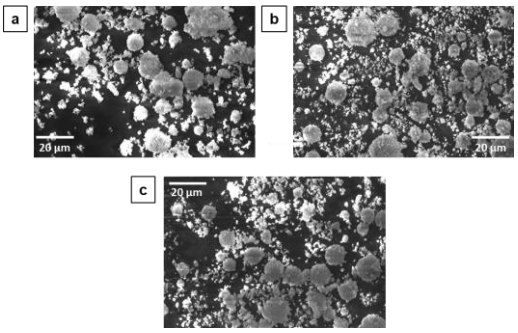

Figure 10: SEM pictures of powders spray-dried in Us1 conditions using the ultrasonic nozzle (a: CR6, b: CR15, c: GE15)

Deagglomeration profiles were also collected for Us1 conditions applying different ultrasound application periods during the wet laser diffraction analysis (Figure 11). The change of the cumulated size distributions versus the ultrasound application time for the three powders is available in supplementary materials (see Figure S3). The size changes for GE15 powder are not drastic since the particle size of the initial powder is close to that of the spray-dried powder. Although clear deagglomeration is noticed for CR6 and CR15 powders, CR6 powder seems to require more time for ultrasonic application to achieve a stabilized size (about 300 s compared to 180 s for CR15 powder).

This would reflect a stronger cohesion of the agglomerates obtained with CR6 powder which presents a narrower initial size distribution.

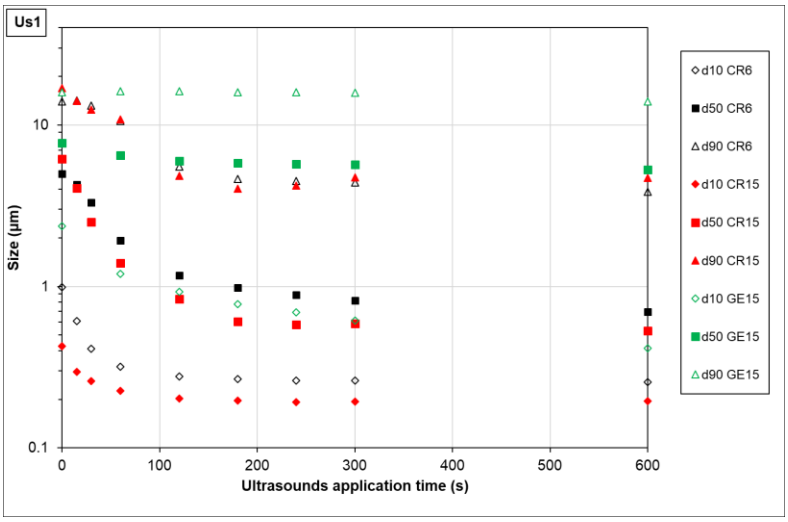

Figure 11: d_{10}, d_{50} and d_{90} evolution for the different powders spray-dried with the ultrasonic nozzle (Us1 conditions)

3.3. Comparison of nozzle technologies

To compare both spray-drying nozzles, Figure 12 assembles results of deagglomeration obtained from tests on CR15 powder under close spray-drying conditions. We can see a clear difference in the case of CR15 powder when spray-dried with a two-fluid nozzle or with an ultrasonic nozzle – under similar conditions of temperature, suspension flow rate and concentration. The process conditions for Us1 and Tf1 are equivalent. Those for Tf4 and Us2 are close; all the process conditions are the same, except for the temperature, which is 140 °C for Us2 and 150°C for Tf4. However, the difference between these temperatures is not enough to have a significant impact on the granules properties and the differences in the particle size and dispersion behaviour were therefore attributed to the change in nozzle geometry. d_{50} obtained with an ultrasonic nozzle is larger, approximately 6 µm (under conditions Us1 or Us2) whereas with a two-fluid nozzle it is 2 µm (under conditions Tf4) and 1.4 µm (under conditions Tf1). With both nozzles, after 600 s of ultrasound the measured d_{50} is very close (0.5 µm). The difference in size is also noteworthy when comparing the SEM images (Figure 13): the larger agglomerates obtained with the two-fluid nozzle (around 5 µm) are smaller than the ones obtained with the ultrasonic nozzle (about 15 µm). This could be due to the different droplet formation process between these two nozzles [47-50]: droplet formation may induce certain droplet velocity that can be high using the two-fluid spraying nozzle and usually is low in ultrasonic spraying device. Concerning the deagglomeration ability, there is a stabilisation of the median size at the same time (about 180 s) for all Tf4, Tf1, and Us1 powders but under Us2 conditions, the minimum size is only obtained after 600 s of ultrasound, suggesting more cohesive agglomerates in this case. However, whatever the conditions, the deagglomeration is considered to be complete since the minimum size is equivalent to that of the initial powder.

According to the results presented in this section, the influence of the initial powder particle size on the feasibility of spray-drying shaping is demonstrated, as well as the advantages of using different types of nozzles. Indeed, the two-fluid nozzle is not suitable for “coarse” powders (in our case, the GE15 powder has a median size of 17 µm) whereas the ultrasonic nozzle seems more suitable. Moreover, ultrasonic atomization produces spherical agglomerates with a higher median size than the

two-fluid nozzle, with a gain noticed of a few micrometres under the same spray-drying conditions (d_{50} going from 2 to 6 µm).

In addition, a significant difference was noticed on the yield of recovered powder, which reached 80% on average with two-fluid nozzle, against 30% with ultrasonic nozzle. The missing powder is located on the walls of the spray column, in the feed pipes, or in the filter sock at the spray outlet.

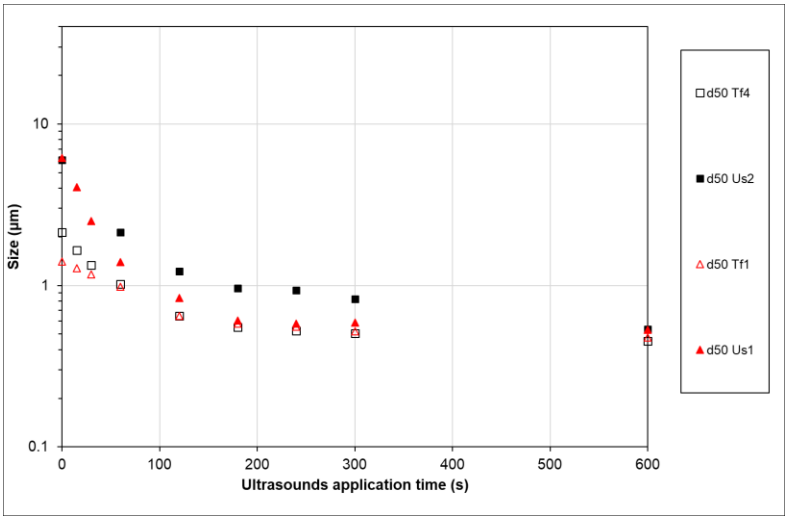

Figure 12: Comparison of d_{50} evolution for CR15 powder spray-dried with both nozzle technologies under close conditions

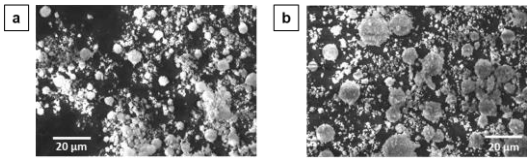

Figure 13: SEM pictures of CR15 powders spray-dried with both nozzle technologies under equivalent conditions (a: Tf1 - two-fluid, b: Us1 - ultrasonic)

3.4. Deagglomeration characterization

In this section, we quantify differences in deagglomeration behaviour and model the rate of deagglomeration. The formula proposed by Schuck et al. [42] (Equation 1) was chosen owing to the noteworthy differences of d_{50} measured with and without dispersion, then adjusted to the size distribution measurements discussed in the previous sections and obtained by wet laser diffraction analysis. Only the results obtained with the ultrasonic nozzle are detailed since the changes in particle size distribution were more significant and so it was easier to distinguish the powders. In order to do this, we transposed the dispersion pressure to the application time of ultrasound into liquid suspension that passes through the analysis cell. The formula (3) is proposed for the deagglomeration rate in percent (DR_{exp}):

$$DR_{exp} = 100 * \frac{d_{50i} - d_{50x}}{d_{50i} - d_{50f}} \quad (3)$$

With:

d_{50i} : the median size of the spray-dried powder without applying ultrasound to the dispersion for wet size measurement

d_{50x} : the median size measured after a given ultrasound application time

d_{50f} : the median size of the raw powder once it no longer evolves (that is considered as the minimum achievable size)

As an example, the deagglomeration rate, calculated with the equation (3) in the case of CR6 and CR15 powders spray-dried with the ultrasonic conditions under conditions Us1, is presented in Figure 14. The deagglomeration rate for both powders follows the same trend. However, as already mentioned in section 3.2, CR6 powder spray-dried with the ultrasonic nozzle takes longer to deagglomerate than CR15. The aim is to express this trend quantitatively as a law of deagglomeration rate versus ultrasonic application time and thus to evaluate the difference in behaviour that can be observed for a characteristic ultrasonic dispersion time.

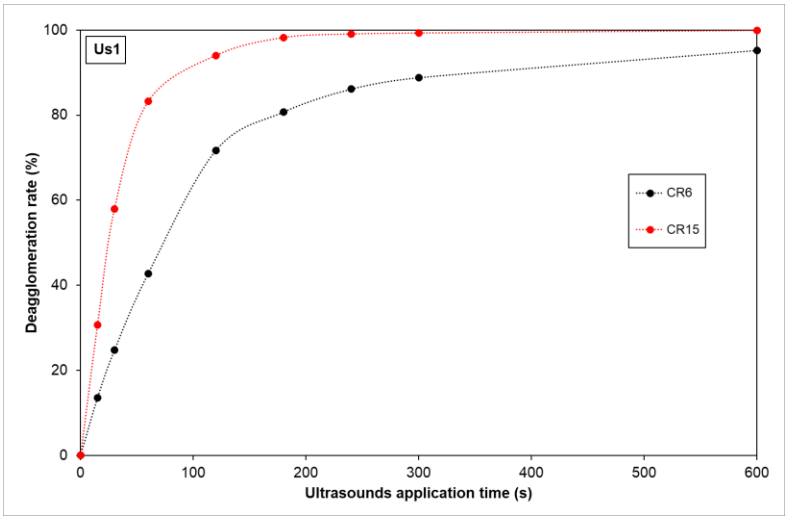

Figure 14: Deagglomeration rates for CR6 and CR15 powders spray-dried in Us1 conditions

The deagglomeration equation (Equation 2) proposed by Parisini et al. [43] is used to fit the experimental curves. In this equation, m, n and t_0 are variable parameters. m is calculated from the "maximal deagglomeration" of spray-dried powder compared to deagglomerated initial powder. It is actually the relation (4) that gives m values. $d_{50_{600s}}$ corresponds to the d_{50} measured for spray-dried powders after 600 s of ultrasound application.

$$m = 100 * \frac{d_{50i} - d_{50_{600s}}}{d_{50i} - d_{50f}} \quad (4)$$

Equation (5), derived from equation (2), is employed to quantify (DR_{mod}) the fitted relative deagglomeration in percent.

$$DR_{mod} = m * \left(1 - e^{-(t/t_0)^n}\right) \quad (5)$$

To determine t_0 and n values, the linear transformation of equation (5) is derived in order to get a linear equation, with DR_{exp} the experimental deagglomeration rate measured as a function of time t:

$$ln\left(ln\left(\frac{m}{m - DR_{exp}}\right)\right) = n * ln(t) - n * \ln(t_0) \quad (6)$$

Equation (6) shows a linear equation with n as the slope and t_0 as the intercept. Figure 15 presents three curves of deagglomeration rate obtained experimentally for CR15 powder (experiments Us1, Us2 and Us3 – dots) and the fitting curves according to our calculations (dotted lines – equation (5)). The fitting curves were calculated giving the minimal error criterion ε, defined as by the least squares method in equation (7):

$$\varepsilon = \frac{\sum_{i=1}^{n}\left[\left(DR_{exp}\right)_i - (DR_{mod})_i\right]^2}{p} \quad (7)$$

Where p represents the number of points measured.

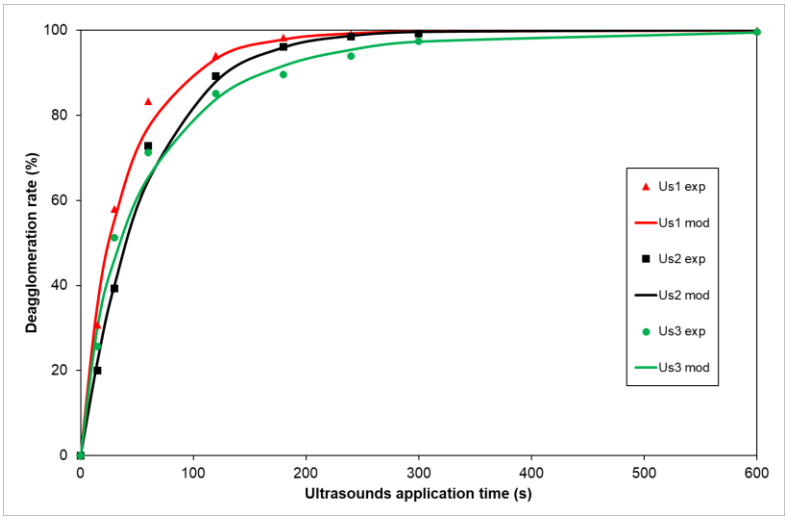

Figure 15: Experimental and modelled deagglomeration rates of CR15 powders spray-dried under various conditions

Whatever the conditions under which the powders were agglomerated, the kinetics of deagglomeration is of order 1 (parameter n varies between 0.78 and 1.02). Three close values were also determined for characteristic time for CR15 powder spray-dried under conditions Us1, Us2 and Us3 (parameter t_0 equals to 38, 58, 50 s, respectively). CR6 (conditions Us1), which experimentally seems to need more ultrasound application time to deagglomerate (Figure 14) presents a higher characteristic time value (t_0 = 99 s). Maximum deagglomeration reached is near 100% for CR15 powder (m = 100%) while CR6 powder stays a few agglomerated (m = 95%). The error criterion calculated from least squares method (ε) is low for all calculations (less than 0.1), showing good quality of the model used to fit the experimental curves. The small differences between the model and experimental curves are probably due to an insufficient number of experimental points between 50 s and 150 s of ultrasound application time. What comes out of these data is a clear difference of deagglomeration time for CR6 and CR15 powders spray-dried under same conditions, while the difference entailed by changing gas temperature and suspension flow rate (within the range tested) is lower.

In addition, similar curves (not reported here) were obtained for the rate of deagglomeration for CR15 powder spray-dried with the two-fluid nozzle under the different conditions Tf1 to Tf5. Whatever the operating conditions, the order of the deagglomeration kinetics remains close to 1 (range 0.8 to 1.2) and the characteristic times vary from 49 to 84 s. Deagglomeration kinetics are therefore slightly slower for powders obtained with the two-fluid nozzle compared to those obtained with the ultrasonic nozzle but this must be put in relation with the size of the agglomerates. The smaller the agglomerates are, the greater the cohesion of the agglomerates [51]. Nevertheless, it is observed that in all cases, the deagglomeration is complete (m close to 100%), which highlights the fragility of agglomerates produced by spray-drying without binder.

Conclusion

The ability of alumina powders to form spherical agglomerates with spray-drying technology relies in particular on their particle size distribution. When using a two-fluid nozzle in the absence of a binder, for example, it was not possible to obtain spherical alumina agglomerates from a coarse-grained powder. The use of an ultrasonic nozzle corrected this problem. In addition, this nozzle increases the size of the spherical agglomerates when spray drying is carried out under the same conditions of slurry concentration, slurry feed rate and gas temperature. This could be a consequence of the different ways of generating the droplets into the drying chamber depending on the nozzle technology used.

The redispersion of agglomerates in liquid phase was analysed by applying variable ultrasound durations during the particle size measurement performed by wet diffraction. Regardless of the alumina powders and spray drying conditions, a similar trend in deagglomeration rate was observed. In the vast majority of cases, the deagglomeration kinetics is of order one and admits a characteristic kinetic time (t_o) which depends mostly on the properties of the powders and to a lesser extent on the nozzle geometry. Deagglomeration is also complete or nearly complete with an ultrasonic application time of less than 600s. The characteristics of the initial powders are then restored, reflecting the brittleness of agglomerates produced by spray-drying without binder.

It seems that the initial particle size and specific surface of the powder play a predominant role in relation to the variation of spray drying operating conditions both in terms of size characteristics and redispersion properties in aqueous solution. Indeed, spray-dried CR6 and CR15 powders, which have similar initial agglomerate median size but differ in specific surface area, behave much more differently when redispersed under ultrasound than CR15 alumina powders spray-dried under different spray conditions within the ranges of variation of the parameters tested (temperature, slurry concentration, slurry feed rate).

Acknowledgements

Scientific and financial support from Orano company are gratefully acknowledged.

References

[1] A. Roosen and H. K. Bowen, 'Influence of Various Consolidation Techniques on the Green Microstructure and Sintering Behavior of Alumina Powders', *J. Am. Ceram. Soc.*, vol. 71, no. 11, pp. 970–977, 1988, doi: 10.1111/j.1151-2916.1988.tb07567.x.

[2] F. F. Lange, 'Powder Processing Science and Technology for Increased Reliability', *J. Am. Ceram. Soc.*, vol. 72, no. 1, pp. 3–15, 1989, doi: 10.1111/j.1151-2916.1989.tb05945.x.

[3] F. F. Lange, B. I. Davis, and I. A. Aksay, 'Processing-Related Fracture Origins: III, Differential Sintering of ZrO2 Agglomerates in Al2O3/ZrO2 Composite', *J. Am. Ceram. Soc.*, vol. 66, no. 6, pp. 407–408, 1983, doi: 10.1111/j.1151-2916.1983.tb10070.x.

[4] D.-M. Liu, J.-T. Lin, and W. H. Tuan, 'Interdependence between green compact property and powder agglomeration and their relation to the sintering behaviour of zirconia powder', *Ceram. Int.*, vol. 25, no. 6, pp. 551–559, Aug. 1999, doi: 10.1016/S0272-8842(97)00094-1.

[5] G. L. Messing, C. J. Markhoff, and L. G. McCoy, 'Characterization of ceramic powder compaction', Jan. 1982, Accessed: Nov. 27, 2019. [Online]. Available: https://pennstate.pure.elsevier.com/en/publications/characterization-of-ceramic-powder-compaction.

[6] K. Sato, H. Abe, M. Naito, T. Hotta, and K. Uematsu, 'Structure of strength-limiting flaws in alumina ceramics made by the powder granule compaction process', *Adv. Powder Technol.*, vol. 17, no. 2, pp. 219–228, Jan. 2006, doi: 10.1163/156855206775992364.

[7] P. Ramavath, M. Swathi, M. Buchi Suresh, and R. Johnson, 'Flow properties of spray dried alumina granules using powder flow analysis technique', *Adv. Powder Technol.*, vol. 24, no. 3, pp. 667–673, May 2013, doi: 10.1016/j.apt.2012.12.006.

[8] S. Cottrino, Y. Jorand, J. Adrien, and C. Olagnon, 'Spray-drying of highly concentrated nano alumina dispersions', *Powder Technol.*, vol. 237, pp. 586–593, Mar. 2013, doi: 10.1016/j.powtec.2012.12.058.

[9] Y. Agniel, 'Rôle des propriétés des granules pour la fabrication de pièces de poudres céramiques granulées sans défaut de compaction', thesis, Lyon, INSA, 1992.

[10] K. Masters, *Spray Drying Handbook*. Longman Scientific & Technical, 1972.

[11] R. A. Youshaw and J. W. Halloran, 'Compaction of spray-dried powders', *Compact. Spray-Dried Powders*, 1982.

[12] A. Wang, Y. Lu, R. Zhu, S. Li, and X. Ma, 'Effect of process parameters on the performance of spray dried hydroxyapatite microspheres', *Powder Technol.*, vol. 191, no. 1, pp. 1–6, Apr. 2009, doi: 10.1016/j.powtec.2008.10.020.
[13] L. Zhang, Y. Li, X. Li, H. Yang, X. Qiao, T. Zhou, Z. Wang, J. Zhang and D. Tang, 'Characterization of spray granulated Nd:YAG particles for transparent ceramics', *J. Alloys Compd.*, vol. 639, pp. 244–251, Aug. 2015, doi: 10.1016/j.jallcom.2015.02.229.
[14] M. Vicent, E. Sánchez, T. Molina, M. I. Nieto, and R. Moreno, 'Comparison of freeze drying and spray drying to obtain porous nanostructured granules from nanosized suspensions', *J. Eur. Ceram. Soc.*, vol. 32, no. 5, pp. 1019–1028, May 2012, doi: 10.1016/j.jeurceramsoc.2011.11.034.
[15] M. Mezhericher, A. Levy, and I. Borde, 'Modelling the morphological evolution of nanosuspension droplet in constant-rate drying stage', *Chem. Eng. Sci.*, vol. 66, no. 5, pp. 884–896, Mar. 2011, doi: 10.1016/j.ces.2010.11.028.
[16] T. Breinlinger, A. Hashibon, and T. Kraft, 'Simulation of the influence of surface tension on granule morphology during spray drying using a simple capillary force model', *Powder Technol.*, vol. 283, pp. 1–8, Oct. 2015, doi: 10.1016/j.powtec.2015.05.009.
[17] H. Minoshima, K. Matsushima, H. Liang, and K. Shinohara, 'Basic Model of Spray Drying Granulation.', *J. Chem. Eng. Jpn.*, vol. 34, no. 4, pp. 472–478, 2001, doi: 10.1252/jcej.34.472.
[18] G. Bertrand, C. Filiatre, H. Mahdjoub, A. Foissy, and C. Coddet, 'Influence of slurry characteristics on the morphology of spray-dried alumina powders', *J. Eur. Ceram. Soc.*, vol. 23, no. 2, pp. 263–271, Feb. 2003, doi: 10.1016/S0955-2219(02)00171-1.
[19] A. Choudhary, P. Ramavath, P. Biswas, N. Ravi, and R. Johnson, 'Experimental Investigation on Flowability and Compaction Behavior of Spray Granulated Submicron Alumina Granules', *Int. Sch. Res. Not.*, 2013, doi: 10.1155/2013/264194.
[20] B. Yu, Y. J. Feng, L. S. Wohn, C. Huang, Y. F. Li, and Z. Jia, 'Spray-drying of alumina powder for APS: effect of slurry properties and drying conditions upon particle size and morphology of feedstock', *Bull. Mater. Sci.*, vol. 34, no. 7, pp. 1653–1661, Dec. 2011, doi: 10.1007/s12034-011-0373-0.
[21] R. G. Frey and J. W. Halloran, 'Compaction Behavior of Spray-Dried Alumina', *J. Am. Ceram. Soc.*, vol. 67, no. 3, pp. 199–203, Mar. 1984, doi: 10.1111/j.1151-2916.1984.tb19742.x.
[22] S. Baklouti, P. Coupelle, T. Chartier, and J. Baumard, 'Compaction Behaviour of Alumina Powders Spray-Dried with Organic Binders', *J. Phys. III*, vol. 6, no. 10, pp. 1283–1291, 1996, doi: 10.1051/jp3:1996186.
[23] A. Stunda-Zujeva, Z. Irbe, and L. Berzina-Cimdina, 'Controlling the morphology of ceramic and composite powders obtained via spray drying – A review', *Ceram. Int.*, vol. 43, no. 15, pp. 11543–11551, Oct. 2017, doi: 10.1016/j.ceramint.2017.05.023.
[24] A. B. D. Nandiyanto and K. Okuyama, 'Progress in developing spray-drying methods for the production of controlled morphology particles: From the nanometer to submicrometer size ranges', *Adv. Powder Technol.*, vol. 22, no. 1, pp. 1–19, Jan. 2011, doi: 10.1016/j.apt.2010.09.011.
[25] S. J. Lukasiewicz, 'Spray-Drying Ceramic Powders', *J. Am. Ceram. Soc.*, vol. 72, no. 4, pp. 617–624, 1989, doi: 10.1111/j.1151-2916.1989.tb06184.x.
[26] A. Stunda-Zujeva, V. Stepanova, and L. Bērziņa-Cimdiņa, 'Effect of spray dryer settings on the morphology of illite clay granules', *Environ. Technol. Resour. Proc. Int. Sci. Pract. Conf.*, vol. 1, p. 216, Jun. 2015, doi: 10.17770/etr2015vol1.200.
[27] A. Dalmoro, A. A. Barba, G. Lamberti, and M. d'Amore, 'Intensifying the microencapsulation process: Ultrasonic atomization as an innovative approach', *Eur. J. Pharm. Biopharm.*, vol. 80, no. 3, pp. 471–477, Apr. 2012, doi: 10.1016/j.ejpb.2012.01.006.
[28] M. O. Panão, A. L. N. Moreira, J. Vicente, and E. Costa, 'Assessment of ultrasonic sprays for spray drying', Conference paper, *17th International Symposium on Application of Laser Techniques to Fluid Mechanics, Lisbon, Portugal*, July 07 – 10, 2014.
[29] F. Tatar Turan, A. Cengiz, and T. Kahyaoglu, 'Evaluation of ultrasonic nozzle with spray-drying as a novel method for the microencapsulation of blueberry's bioactive compounds', *Innov. Food Sci. Emerg. Technol.*, vol. 32, pp. 136–145, Dec. 2015, doi: 10.1016/j.ifset.2015.09.011.
[30] W. Klaypradit and Y.-W. Huang, 'Fish oil encapsulation with chitosan using ultrasonic atomizer', *LWT - Food Sci. Technol.*, vol. 41, no. 6, pp. 1133–1139, Jul. 2008, doi: 10.1016/j.lwt.2007.06.014.
[31] P. P. Luz, A. M. Pires, and O. A. Serra, 'A low-cost ultrasonic spray dryer to produce spherical microparticles from polymeric matrices', *Quimica Nova*, 2007, doi: http://dx.doi.org/10.1590/S0100-40422007000700041.
[32] B. Bittner and T. Kissel, 'Ultrasonic atomization for spray drying: a versatile technique for the preparation of protein loaded biodegradable microspheres', *J. Microencapsul.*, vol. 16, no. 3, pp. 325–341, Jan. 1999, doi: 10.1080/026520499289059.

[33] T. Schneider and K. Jensen, ‘Combined Single-Drop and Rotating Drum Dustiness Test of Fine to Nanosize Powders Using a Small Drum’, *Ann. Occup. Hyg.*, vol. 52, pp. 23–34, Jan. 2008, doi: 10.1093/annhyg/mem059.
[34] S. Jaffari, B. Forbes, E. Collins, D. J. Barlow, G. P. Martin, and D. Murnane, ‘Rapid characterisation of the inherent dispersibility of respirable powders using dry dispersion laser diffraction’, *Int. J. Pharm.*, vol. 447, no. 1, pp. 124–131, Apr. 2013, doi: 10.1016/j.ijpharm.2013.02.034.
[35] J. A. Kurkela, D. P. Brown, J. Raula, and E. I. Kauppinen, ‘New apparatus for studying powder deagglomeration’, *Powder Technol.*, vol. 180, no. 1, pp. 164–171, Jan. 2008, doi: 10.1016/j.powtec.2006.10.032.
[36] M. Ghadiri, Z. Zhang, ‘Impact attrition of particulate solids. Part 1 : A theoretical model of chipping’, *Chem. Eng. Sci.*, vol. 57, no. 17, pp. 3659-3669, 2002. doi:10.1016/S0009-2509(02)00240-3
[37] R. Moreno, M. Ghadiri, and S. J. Antony, ‘Effect of the impact angle on the breakage of agglomerates : A numerical study using DEM’, *Powder Technol.*, vol. 130, *no.* 1, pp. 132-137, 2003. doi:10.1016/S0032-5910(02)00256-5
[38] R. Moreno, M. Ghadiri, ‘Mechanistic analysis and computer simulation of impact breakage of agglomerates : Effect of surface energy’, *Chem. Eng. Sci.*, vol. 61, no. 8, pp. 2476-2481, 2006. doi:10.1016/j.ces.2005.11.019
[39] P. Mahr and B. Halbedel, ‘Characterisation of the deagglomeration behaviour of nanoscaled barium hexaferrite powders by measurement of electrokinetic effects’, *Mater. Werkst.*, vol. 37, no. 11, pp. 933–936, Nov. 2006, doi: 10.1002/mawe.200600081.
[40] F. Wang, I. Tzanakis, D. Eskin, J. Mi, and T. Connolley, ‘In situ observation of ultrasonic cavitation-induced fragmentation of the primary crystals formed in Al alloys’, *Ultrason. Sonochem.*, vol. 39, pp. 66–76, Nov. 2017, doi: 10.1016/j.ultsonch.2017.03.057.
[41] O. Kudryashova, A. Vorozhtsov, and P. Danilov, ‘Deagglomeration and Coagulation of Particles in Liquid Metal Under Ultrasonic Treatment’, *Archives of Acoustics*, vol. 44, no. 3, pp. 543–549, Jun. 2019. doi: 10.24425/aoa.2019.129269.
[42] P. Schuck, A. Dolivet, and R. Jeantet, *Les poudres laitières et alimentaires*. 2012.
[43] I. Parisini, J. L. Collett, and D. Murnane, ‘Mathematical approach for understanding deagglomeration behaviour of drug powder in formulations with coarse carrier’, *Asian J. Pharm. Sci.*, vol. 10, no. 6, pp. 501–512, Dec. 2015, doi: 10.1016/j.ajps.2015.08.007.
[44] M. Avrami, ‘Granulation, Phase Change, and Microstructure Kinetics of Phase Change. III’, *J. Chem. Phys.*, vol. 9, no. 2, pp. 177–184, Feb. 1941, doi: 10.1063/1.1750872.
[45] L. Liang, L. Wang, A. V. Nguyen, G. Xie, ‘Heterocoagulation of alumina and quartz st udied by zeta potential distribution and particle size distribution measurements’, *Powder Technology*, vol 309, p.1-12, March 2017, doi: 10.1016/j.powtec.2016.12.054.
[46] J. Sauter, ‘Die Grössenbestimmung der im Gemischnebel von Verbrennungskraftmaschinen vohrhandenen Brennstoffteilchen’, *VDI-Verlag* 1926.
[47] J.J. O'Sullivan, E.A. Norwood, J.A. O'Mahony, A.L. Kelly, ‘Atomisation technologies used in spray drying in the dairy industry: A review’, Journal of food engineering, vol 243, p. 57-69, 2019, doi.org/10.1016/j.jfoodeng.2018.08.027.
[48] M. Mezhericher, J. K. Nunes, J. Guzowski, H. A. Howard, ‘Aerosol-Assisted Synthesis of Submicron Particles at Room Temperature Using Ultra-Fine Liquid Atomization’, *Chemical Engineering Journal*, vol 346, pp. 606-620, April 2018, doi: 10.1016/j.cej.2018.04.054.
[49] Sono-Tek brochure, available on : https://pdf4pro.com/cdn/ultrasonic-spray-nozzle-systems-sono-tek-b47e1.pdf
[50] R. Wisniewski, ‘Spray Drying Technology Review’, 45th International Conference on Environmental Systems, Washington, 12-16 July 2015.
[51] K. Kendall, ‘Adhesion: molecules and mechanics’, *Sciences*, vol 263, no. 5154, pp. 1720-1725, 1994, doi: 10.1126/science.263.5154.1720.

Supplementary material

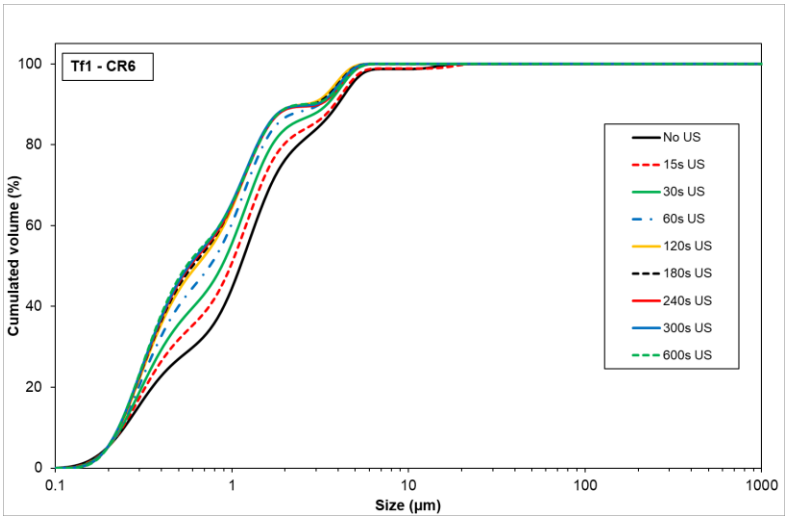

Figure S1: Impact of ultrasound application on the dispersion of CR6 powder spray-dried (Tf1 conditions): evolution of size distribution

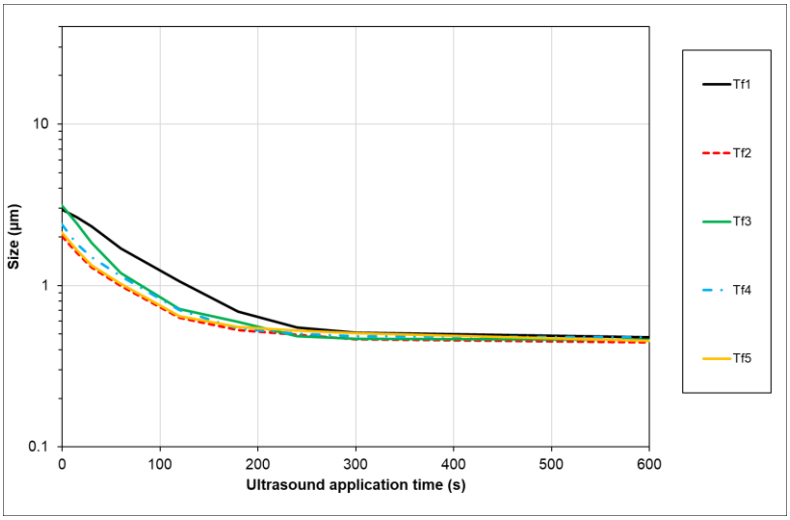

Figure S2: d_{50} change versus the ultrasound application time for the CR15 powder spray-dried under various operating conditions

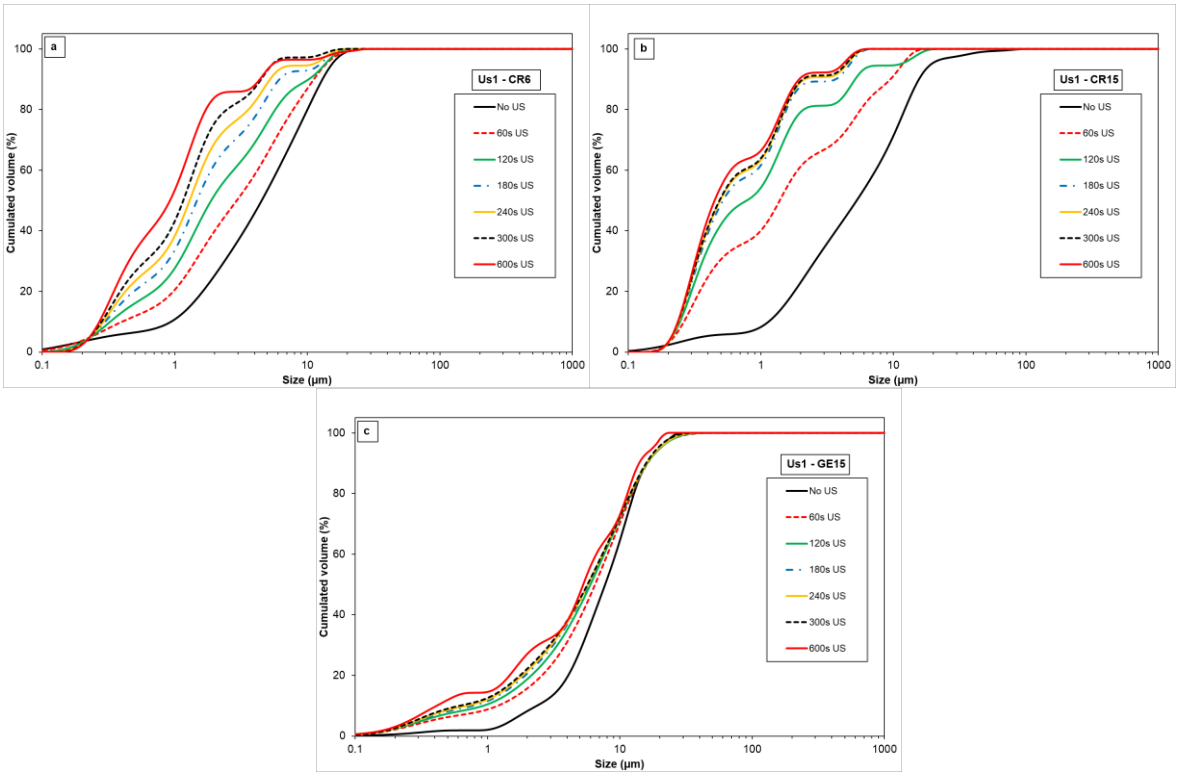

Figure S3: Impact of ultrasound application on the dispersion of the three powders spray-dried under Us1 conditions: evolution of size distribution (a: CR6, b: CR15, c: GE15)

List of Figures

Supplementary Material

List of Tables